

The role of buoyancy reversal in turbidite deposition and submarine fan geometry

Elisabeth Steel¹, James Buttles², Alexander R. Simms¹, David Mohrig², and Eckart Meiburg³

¹Department of Earth Science, University of California, Santa Barbara, California 93106, USA

²Jackson School of Geosciences, University of Texas at Austin, C9000, Austin, Texas 78712, USA

³Department of Mechanical Engineering, University of California, Santa Barbara, California 93106, USA

ABSTRACT

Although recent work has shown that changing interstitial fluid density within turbidity currents is a frequently overlooked factor affecting the texture and internal architecture of turbidites, little is known about its influence on submarine fan morphology. Here we present the results of three-dimensional flume experiments of turbidity currents that clearly demonstrate the role of low-density interstitial fluid, in combination with sediment concentration and basin gradient, on submarine fan geometry. The experiments show that turbidity currents with reversing buoyancy, and their resulting deposits, are narrower than those that remain ground hugging. Furthermore, wider deposits result from increases in sediment concentration and/or basin-floor gradient. We also propose that Taylor-Görtler vortices associated with currents traveling over a break in slope may lead to the deposition of wider lobes compared with those traveling over a constant gradient.

INTRODUCTION

Ancient submarine fans serve as prolific hydrocarbon reservoirs and provide records of climatic and tectonic activity. The economic recovery of hydrocarbons and accurate interpretation of the geologic record rely on the understanding of factors that control fan morphology and architecture. Basin configuration, sediment supply, and antecedent topography are often cited as factors in controlling the geometry of submarine fan lobes (e.g., Normark and Piper, 1991; Reading and Richards, 1994; Fernandez et al., 2014). However, gravity current characteristics such as sediment concentration and the relationship between current density and ambient water density may also significantly affect the morphology of a submarine fan.

Turbidity currents can be classified as ground-hugging currents or lofting currents (Fig. 1) (Meiburg and Kneller, 2010). Lofting, or buoyancy reversal, occurs when an initially ground-hugging turbulent underflow becomes less dense than the surrounding fluid and rises from the basin floor. Despite an abundance of fluid dynamics studies describing lofting, few geologists have investigated its impact on turbidite systems (e.g., Hurzeler et al., 1995; Huppert, 1998; Pritchard and Gladstone, 2009; Zavala and Arcuri, 2016; Steel et al., 2016). Lofting significantly alters the spreading geometry of submarine currents and the extent of their deposits, and should no longer be overlooked in the context of submarine deposition. The purpose of this paper is to use a three-dimensional experimental model to examine

how lofting, basin-floor gradient, and sediment concentration affect turbidity currents and submarine fan geometry.

BACKGROUND

The relationship between ambient water density, interstitial water density, and bulk current density plays a critical role in the evolution of a turbidity current. In the case of a current with relatively light interstitial fluid, bulk current density exceeds ambient water density due to suspended sediment, and a dense underflow travels across the basin floor. The current remains ground hugging as long as bulk density exceeds the surrounding water density (Sparks et al., 1993). As the current progresses, bulk current density may decrease by settling of sediment, or may increase by entrainment of sediment or ambient water. If sediment settles from suspension more rapidly than replacement of interstitial fluid with ambient water, bulk flow density will lighten until it reaches a point of reversing buoyancy. At this point, a buoyant plume will rise from the basin floor (Sparks et al., 1993; Sequeiros et al., 2009). These conditions occur in nature when fresh, sediment-laden rivers meet ocean basins or when turbidity currents initiated in warm, shallow-water environments travel into deeper and colder water (Sparks et al., 1993). Previous studies have focused on understanding two-dimensional aspects of buoyancy reversal, such as spreading rate of flow fronts (Hurzeler et al., 1995), and lift-off points (Sparks et al., 1993; Hogg et al., 1999; Sequeiros et al., 2009; Stevenson and Peakall, 2010), but few studies

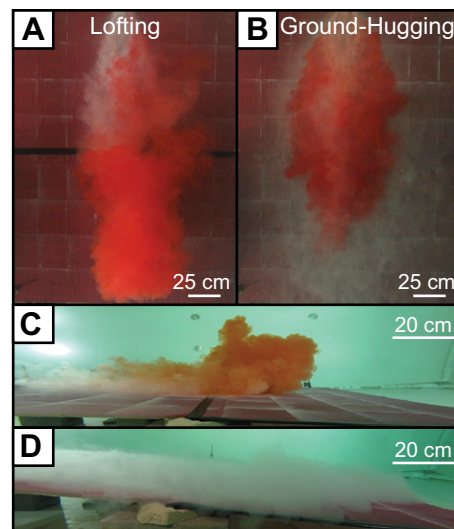


Figure 1. A comparison of a lofting turbidity current (run G) and a ground-hugging turbidity current (run H) with similar initial sediment concentrations, discharge, and bottom slopes. **A:** Overhead photo taken during experiment G. Red dye was injected into the currents to enhance visibility. The current in A contained light interstitial fluid, and a buoyant plume rose along the head and the edges, limiting both the longitudinal and lateral spreading. **B:** Overhead photo taken during experiment H. The current in B remained ground hugging and was wider than the lofting current. **C, D:** Side views of the lofting (C) and ground-hugging (D) currents taken from a camera within the tank show the contrasts between the width and heights of lofting versus ground-hugging currents.

have explored the effects of buoyancy reversal on lateral spreading of flows and its impact on three-dimensional deposit geometry (Zavala et al., 2011).

Ground-hugging currents spread as a logarithmic function of time, and the rate of lateral spreading decreases as slope angle increases (Alavian, 1986; Choi and Garcia, 2001). Buoyancy reversal is likely to alter the spreading rates of currents, and may prevent them from reaching their predicted maximum width (Zavala et al., 2011). Furthermore, the decrease in velocity at a slope break can lead to rapid sedimentation,

which may enhance or initiate lofting. Therefore, a discussion of lofting dynamics is incomplete without an understanding of the links between lofting and basin geometry.

EXPERIMENTAL SETUP

In this study we conducted 12 experimental turbidity currents, 9 of which lofted (Table DR1 in the GSA Data Repository¹). Experiments were performed on a 2.4-m-long by 1.8-m-wide tilted ramp inside the Experimental Deep Water Basin at the University of Texas (Austin, Texas). The basin is 4 m wide, 8 m long, and 2 m deep (Fig. DR1 in the Data Repository). Video cameras recorded currents from inside the tank (underwater), from outside the tank through an observation window, and from a raised platform (see footnote 1). Overhead photos were taken every 10 s during runs. Density contrasts between interstitial current water and ambient tank water were achieved by heating the interstitial water to 31 °C and keeping ambient water at 23 °C. Plastic sediment with a particle size distribution d_{50} grain size of 206 μm and density of 1.15 g/cm^3 was mixed with the warm interstitial water and piped onto the submerged ramp. Currents were run across three ramp geometries: 5° slope to flat, constant 5° slope, and constant 8° slope. On each ramp geometry, currents with warm interstitial water were conducted with 1.5%, 2%, and 3% sediment concentration. Currents with the same ambient and interstitial water densities were conducted with 1.6% sediment concentration in order to allow comparisons between ground-hugging and lofting currents of similar sediment concentrations as well as those of the same bulk densities (Table DR1). Bulk inlet discharge was 278.1 cm^3/s and currents were run for 12 min. After the completion of each run, the deposit was scanned using a high-resolution underwater laser scanner (Fig. DR2). The water was drained and the tank cleaned before running subsequent currents.

Lofting of flow margins in each run was identified using a combination of overhead photos and side videos. The maximum flow width as a function of time was measured from a sequence of overhead photos (Figs. DR3 and DR4). Lofting was identified when a current stopped widening, defined here by four successive measurements of the same width during

a run. Ground-hugging currents continuously widened with time, eventually becoming wider than the ramp.

RESULTS

All currents with light interstitial fluid were initially ground hugging (bed attached) on all ramp geometries (Fig. 2A). Lofting initiated along the current fronts and lateral margins while the interior remained bed attached (Fig. 2B). Lofting along the margins induced an inward flow of ambient fluid, which first reduced the current spreading rate and eventually stopped lateral spreading (Fig. 2C). This is in contrast to ground-hugging currents, which continued to spread and flow over ramp edges (Fig. 1B). During lofting, the rising plume maintained both forward and upward momentum, carrying with it suspended sediment. Gradually, the plume spread along the free water surface in all directions.

A comparison of the maximum half-width through time for lofting and ground-hugging currents clearly shows the width-limiting nature of lofting (Fig. 3A; Figs. DR3 and DR4).

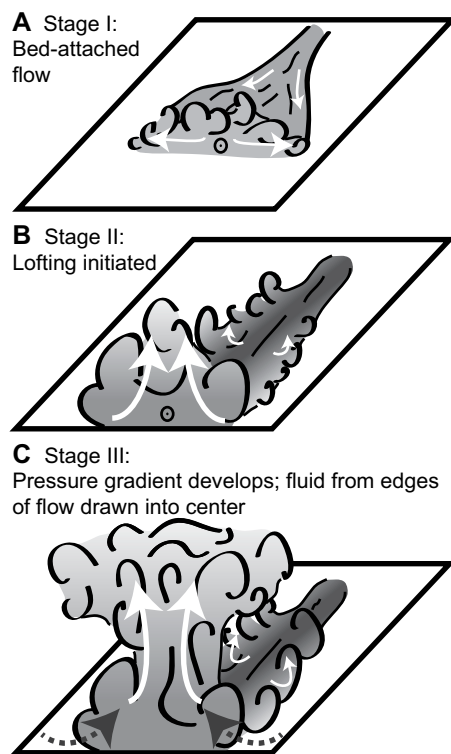


Figure 2. Schematic diagram of the lofting process. A: In stage 1, the current is ground hugging and spreads both laterally and longitudinally. B: As sediment is deposited from the current, bulk density decreases and the current becomes buoyant and lofts at the front and lateral margins. C: A low-pressure zone develops below the lofting portions of the current, creating pressure gradients that slow and then stop longitudinal and lateral spreading. Sediment that remains in suspension during lofting settles from the plume over a broad area.

Following the methods of Choi and Garcia (2001), half-width lengths and times were normalized by characteristic plume length and time scales (l_p, t_p), which approximate the length and time scales at which a density current transitions from jet (momentum) dominated to buoyancy (plume) dominated flow. The ground-hugging currents spread laterally through time as predicted by Choi and Garcia (2001) (run H; Fig. 3A). In contrast, lofting currents spread laterally with time until reaching a constant half-width that was then maintained for the remainder of the flow (Fig. 3A). The maximum half-width length and time to lofting increased with higher initial suspended sediment concentration (Fig. 3A).

The shape of deposits from lofting currents is distinct from those formed by currents that remained ground hugging; lofting currents formed narrower deposits than ground-hugging currents of similar or greater sediment concentration in all cases (Fig. 3B; Fig. DR5). Once the current lofted, a thin layer of sediment settled from the plume over a wide area, resulting in an initially narrow deposit that broadens in its most distal reaches. The ground-hugging current on the 8° ramp (run L) had a lower spreading rate than the ground-hugging current on the 5° ramp (run H) and therefore a narrower current and deposit. This confirms predictions that steeper gradients result in lower rates of lateral spreading in ground-hugging flows (Alavian, 1986).

Lofting currents with higher sediment concentrations began to loft later, and were therefore wider and deposited wider lobes (Fig. 3). In addition, flows on the 8° ramp had a higher frontal velocity, underwent buoyancy reversal farther basinward, and deposited wider lobes than those traveling across the 5° and 5° to flat ramps.

DISCUSSION

Dynamics of Buoyancy Reversal

Despite the importance of predicting the geometry of sand bodies, particularly for the economic extraction of hydrocarbons, little is known about the three-dimensionality of lofted-current deposits. Observing buoyancy reversal in a three-dimensional setting allows the effects of light interstitial fluid on lateral spreading of currents to be seen, as well as the resulting changes in length-to-width ratios of their deposits.

The flow margins of currents with light interstitial fluid are more dilute than the flow center, and therefore have a lower contrast between the flow and ambient water densities. Because of this density gradient, as sediment settles from suspension and bulk current density decreases, current margins reach a point of neutral buoyancy before the current interior. Once current margins become buoyant, lateral spreading of the current ceases and vortices form, pulling fluid from the edges of the current inward

¹GSA Data Repository item 2017009, Table DR1 (experimental conditions), Figure DR1 (diagram of tank setup), Figure DR2 (deposit thickness maps), Figure DR3 (spreading rates on 5° to flat and 8° ramps), Figure DR4 (comparison of spreading rates on steep vs. shallow ramps), Figure DR5 (sediment concentration vs. lobe width), and Figure DR6 (schematic of Taylor-Görtler vortices), is available online at www.geosociety.org/pubs/ft2016.htm, or on request from editing@geosociety.org. Videos of lofting and ground-hugging currents from this study are available on the Sediment Experimentalists Network (SEN) Knowledge Base at sedexp.net.

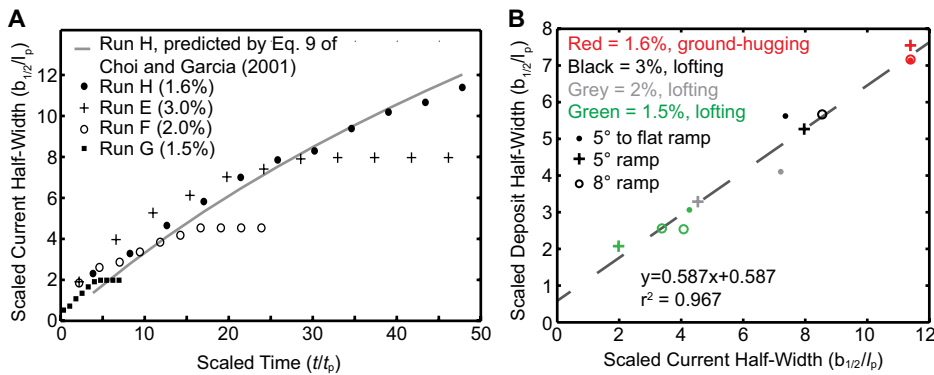


Figure 3. A: Comparison of scaled maximum current half-width with scaled time for runs on the 5° ramp. Half-width ($b_{1/2}$) and time are normalized by characteristic plume length and time scales l_p and t_p , using equations (Eq.) of Choi and Garcia (2001, their equations 3 and 4). The solid line is the empirically predicted fit for the lateral spreading of a ground-hugging current (black dots) using the methods of Choi and Garcia (2001). Lofting currents spread until they begin to loft, at which point they maintain a constant width. Currents with higher sediment concentrations loft later, and are therefore wider. B: Comparison of current half-width and deposit half-width. There is a strong linear relationship between current half-width and deposit half-width. Despite having a low sediment concentration, ground-hugging flows (red) are the widest and produce the widest deposits. Current half-widths were measured using overhead photos taken every 10 s. Lofted-current deposit widths were measured from cross-sectional laser profiles as the distance between inflection points on each side of the deposit. Ground-hugging deposit margins thinned below the laser resolution but were visually apparent (Fig. DR2 [see footnote 1]). Therefore, ground-hugging deposit widths were determined using overhead photos and measured as the width at which the light-colored sediment could no longer be identified on top of the dark-colored ramp.

and upward (Fig. 2). In addition to the rise of the current margins, the current head expands significantly as forward velocity of the current decreases. The vertical expansion at the head of a ground-hugging turbidity current is due to shear instabilities causing Kelvin-Helmholtz billows and entrainment of ambient water (Britter and Simpson, 1978). However, the expansion at the head of the currents with light interstitial fluid is likely to result from loss of sediment, causing decreased current density and rising of a buoyant plume. If significant entrainment of ambient water occurred, interstitial water would be replaced and currents would continue as ground hugging rather than lofting. When the current lifts off from the basin floor, any sediment left in suspension rises with it and is distributed over a broad area. Depending on local conditions, the rising plume may be carried away by cross-currents or may deposit a thin layer of fine sediment on top of the narrow lobe emplaced by the bed-attached portion of the current.

Effects of Sediment Concentration and Ramp Gradient on Deposit Geometry

A strong correlation is observed between current width and deposit width, and factors that affect lateral spreading of currents will similarly affect deposit geometry (Fig. 3B). Currents with higher sediment concentrations produced wider deposits and began to loft farther basinward than flows with lower sediment concentrations. The higher sediment concentration results in higher bulk current density, and therefore a greater

contrast between the initial current and ambient water density. For the current to reach a point of neutral or positive buoyancy, a current with high suspended sediment concentration must deposit more sediment and travel farther across the basin floor before lofting. Thus the current will have more time to spread laterally before lofting, resulting in an overall wider flow and deposit. In natural systems, sediment grain size will also play a role in the lofting distance and currents with high concentrations of mud-sized sediment may loft much later or not at all due to hindered sediment settling (Zavala and Arcuri, 2016).

Lofting flows traveling across steeper ramp gradients result in farther basinward lofting points and wider deposits. This behavior occurs because currents moving across steeper gradients travel a greater distance basinward and spread farther laterally in a comparable amount of time preceding lofting (Fig. DR4). However, because ground-hugging currents have lower rates of lateral spreading on steeper ramps (Alavian, 1986), and because lofting will not limit their maximum width, ground-hugging currents on steep ramps should produce narrower deposits than ground-hugging currents on shallow ramps, as seen in run L on the 8° ramp compared to run H on the 5° ramp (Table DR1; Fig. 3B).

In all lofting cases, the 5° to flat deposits were wider than the 5° ramp deposits. The effect of a break in slope on deposit width is likely a reflection of Taylor-Görtler vortices (Taylor, 1921; Pantón, 1984). When a current travels over a concave surface, and is relatively thick compared to the radius of curvature of

the surface, centrifugal force begins to act on the fluid and pushes the current down into the basin floor (Fig. DR6). Centrifugal force acts more strongly on faster moving fluid particles, meaning that it will be greater on particles in the central portion of the current than on the slower moving particles near the base or top of the current. This downward-directed centrifugal force forms Taylor-Görtler vortices, which effectively cause the current to spread laterally as an upper part of the current is pushed down and lower flow particles are pushed out (Taylor, 1921; Pantón, 1984). The original goal of designing a ramp with a slope break was to explore its effects on the location of the lofting point. However, although not measured directly, the widening effects of Taylor-Görtler vortices likely play a more significant role in flow dynamics of these experimental currents. The effects of Taylor-Görtler vortices may be enhanced by a decrease in velocity at the slope break, causing current competency to decrease and promoting sediment deposition. The Taylor-Görtler vortices do not appear to have such a strong effect on ground-hugging flows, perhaps because all flows overran the platform boundary and never achieved a true maximum width.

Both Taylor-Görtler vortices (5° to flat ramp) and a basinward shift in the lofting point (8° ramp) appear to cause wider currents, making a comparison between the two ramp geometries complex. Other factors beyond the scope of this study, such as flow inertia and grain-size distribution, may also affect lofting and current width. However, this study shows that the primary width-limiting process is buoyancy reversal, and that within lofting currents the location of the lift-off point, which adjusts due to changes in sediment concentration or ramp geometry, controls the ultimate width of the deposit.

Comparison to Ancient and Modern Deposits

Based on this study and previous work on lofting turbidity currents, lofted deposits are expected to have narrow lobes with abrupt frontal and lateral terminations (Gladstone and Pritchard, 2010). Previous studies showed that the internal architecture of lofted deposits is expected to consist of a fines-depleted basal layer, deposited by the bed-attached flow, and a fines-enriched mantle, deposited by the lofted plume (Walker and McBroom, 1983). The fines-enriched mantle may not be present if the plume is carried far from its lift-off point. The basal layer is rapidly deposited by the bed-attached portion of the current once buoyancy reversal begins, resulting in a bed that may more closely resemble a sandy debrite (Shanmugam, 1996; Amy et al., 2005) rather than the typical Bouma-type features associated with ground-hugging turbidity currents (Steel et al., 2016). Lofting currents frequently contain river-derived

plant fragments that settle from the lofted plume more slowly than clastic material, resulting in lofted rhythmites composed of sand-silt couplets bounded by thin layers of plant debris (Zavala et al., 2011).

Evidence for turbidites with reversing buoyancy can be found in both modern and ancient turbidite successions around the world. The shelf of the Santa Barbara Channel offshore southern California contains at least six Holocene fans built by hyperpycnal currents (Warrick et al., 2013). The lobes within these fans are narrow, contain distinct margins, and are composed of well-sorted, structureless sand, indicating that the hyperpycnal currents were modified by buoyancy reversal (Steel et al., 2016). In another case, the Middle Jurassic Los Molles Formation of the Neuquén Basin in western Argentina, which is composed of slope and basin-floor deposits, contains upper slope, river-derived turbidites with partial Bouma sequences, as well as occurrences of enigmatic beds that are composed of well-sorted, medium-grained sandstones that are occasionally flat and thickly laminated (Paim et al., 2010; R. Steel, 2016, personal commun.). Individual beds of this type on the slope are ~40 m wide, and are better sorted and significantly narrower than the majority of the turbidites in the lower slope and basin-floor succession (Shin, 2015). Their well-sorted nature and narrow geometry suggest that these unusual beds may be another example of deposition from river-derived turbidity currents with reversing buoyancy.

CONCLUSIONS

Buoyancy reversal is an overlooked process in turbidites. The distinction between ground-hugging and lofting turbidity currents is not pedantic, as it affects the length-to-width ratios of individual sandbodies and the degree of sediment sorting within beds. Ocean stratification leads to conditions in which the fluid within a turbidity current may be less dense than the surrounding ambient water, meaning that buoyancy reversal could play a role in the evolution of the current if suspended sediment settles relatively quickly. Shelf-edge deltaic systems feeding freshwater hyperpycnal currents directly onto the continental slope create ideal conditions for currents with reversing buoyancy.

Other factors such as basin-floor gradient and sediment concentration can alter submarine fan geometry, and disentangling various flow characteristics from the ultimate geometry of turbidites is a difficult task. However, this study provides data intended to advance this understanding of how factors such as sediment concentration, basin configuration, and fluid density control deposit morphology.

ACKNOWLEDGMENTS

Acknowledgment is made to the Donors of the American Chemical Society Petroleum Research Fund for support of this research. This work was also supported in part by a Geological Society of America Graduate Student Research Grant and the University of Texas CSU RioMAR Industry Consortium.

REFERENCES CITED

- Alavian, V., 1986, Behavior of density currents on an incline: *Journal of Hydraulic Engineering*, v. 112, p. 27–42, doi:10.1061/(ASCE)0733-9429(1986)112:1(27).
- Amy, L.A., Talling, P.J., Peakall, J., Wynn, R.B., and Arzola Thynne, R.G., 2005, Bed geometry used to test recognition criteria of turbidites and (sandy) debrites: *Sedimentary Geology*, v. 179, p. 163–174, doi:10.1016/j.sedgeo.2005.04.007.
- Britter, R.E., and Simpson, J.E., 1978, Experiments on the dynamics of a gravity current head: *Journal of Fluid Mechanics*, v. 88, p. 223–240, doi:10.1017/S0022112078002074.
- Choi, S.U., and Garcia, M.H., 2001, Spreading of gravity plumes on an incline: *Coastal Engineering Journal*, v. 43, p. 221–237, doi:10.1142/S0578563401000359.
- Fernandez, R.L., Cantelli, A., Pirmez, C., Sequeiros, O., and Parker, G., 2014, Growth patterns of subaqueous depositional channel lobe systems developed over a basement with a downdip break in slope: Laboratory experiments: *Journal of Sedimentary Research*, v. 84, p. 168–182, doi:10.2110/jsr.2014.10.
- Gladstone, C., and Pritchard, D., 2010, Patterns of deposition from experimental turbidity currents with reversing buoyancy: *Sedimentology*, v. 57, p. 53–84, doi:10.1111/j.1365-3091.2009.01087.x.
- Hogg, A.J., Huppert, H.E., and Hallworth, M.A., 1999, Reversing buoyancy of particle-driven gravity currents: *Physics of Fluids*, v. 11, 2891, doi:10.1063/1.870147.
- Huppert, H.E., 1998, Quantitative modelling of granular suspension flows: *Royal Society of London Philosophical Transactions*, v. 356, p. 2471–2496, doi:10.1098/rsta.1998.0282.
- Hurzeler, B.E., Ivey, G.N., and Imberger, J., 1995, Spreading model for a turbidity current with reversing buoyancy from a constant-volume release: *Marine and Freshwater Research*, v. 46, p. 393–408, doi:10.1071/MF9950393.
- Meiburg, E., and Kneller, B., 2010, Turbidity currents and their deposits: *Annual Review of Fluid Mechanics*, v. 42, p. 135–156, doi:10.1146/annurev-fluid-121108-145618.
- Normark, W.R., and Piper, D.J.W., 1991, Initiation processes and flow evolution of turbidity currents: Implications for the depositional record, in Osborne, R.H., ed., *From shoreline to abyss: Contributions in marine geology in honor of Francis Parker Shepard*: Society for Sedimentary Geology Special Publication 46, p. 207–230, doi:10.2110/pec.91.09.0207.
- Paim, P.S.G., Lavina, E.L.C., Faccini, U.F., Silveira, A.S., Leanza, H., and d'Avila, R.S.F., 2010, Fluvial-derived turbidites in the Los Molles formation (Jurassic of the Neuquén basin): Initiation, transport, and deposition, in Slatt, R.M., and Zavala, C., eds., *Sediment transfer from shelf to deep water—Revisiting the delivery system*: American Association of Petroleum Geologists Studies in Geology 61, p. 95–116, doi:10.1306/13271252St613437.
- Panton, R.L., 1984, *Incompressible flow*: New York, John Wiley & Sons, 780 p.
- Pritchard, D., and Gladstone, C., 2009, Reversing buoyancy in turbidity currents: Developing a hypothesis for flow transformation and for deposit facies and architecture: *Marine and Petroleum Geology*, v. 26, p. 1997–2010, doi:10.1016/j.marpetgeo.2009.02.010.
- Reading, H.G., and Richards, M., 1994, Turbidite systems in deep-water basin margins classified by grain size and feeder system: *American Association of Petroleum Geologists Bulletin*, v. 78, p. 792–822.
- Sequeiros, O.E., Cantelli, A., Viparelli, E., White, J.D.L., Garcia, M.H., and Parker, G., 2009, Modeling turbidity currents with nonuniform sediment and reverse buoyancy: *Water Resources Research*, v. 45, W06408, doi:10.1029/2008WR007422.
- Shanmugam, G., 1996, High-density turbidity currents: Are they sandy debris flows?: *Journal of Sedimentary Research*, v. 66, p. 2–10, doi:10.1306/D426828E-2B26-11D7-8648000102C1865D.
- Shin, M., 2015, Architecture of coarse grained (conglomeratic) deep water lobes at the base of a sandstone dominated fan, Jurassic Los Molles Formation, Neuquen Basin, Argentina [M.S. thesis]: Austin, University of Texas at Austin, 116 p.
- Sparks, R.S.J., Bonnetcaze, R.T., Huppert, H.E., Lister, J.R., Hallworth, M.A., Mader, H., and Phillips, J., 1993, Sediment-laden gravity currents with reversing buoyancy: *Earth and Planetary Science Letters*, v. 114, p. 243–257, doi:10.1016/0012-821X(93)90028-8.
- Steel, E., Simms, A.R., Warrick, J., and Yokoyama, Y., 2016, Highstand shelf fans: The role of buoyancy reversal in the deposition of a new type of shelf sand body: *Geological Society of America Bulletin*, doi:10.1130/B31438.1.
- Stevenson, C.J., and Peakall, J., 2010, Effects of topography on lofting gravity flows: Implications for the deposition of deep-water massive sands: *Marine and Petroleum Geology*, v. 27, p. 1366–1378, doi:10.1016/j.marpetgeo.2010.03.010.
- Taylor, G.I., 1921, Experiments with rotating fluids: *Royal Society of London Proceedings*, ser. A, v. 100, p. 114–121, doi:10.1098/rspa.1921.0075.
- Walker, G.P., and McBroome, L.A., 1983, Mount St. Helens 1980 and Mount Pelée 1902—Flow or surge?: *Geology*, v. 11, p. 571–574, doi:10.1130/0091-7613(1983)11<571:MSHAMP>2.0.CO;2.
- Warrick, J.A., Simms, A.R., Ritchie, A., Steel, E., Dartnell, P., Conrad, J.E., and Finlayson, D.P., 2013, Hyperpycnal plume-derived fans in the Santa Barbara Channel, California: *Geophysical Research Letters*, v. 40, p. 2081–2086, doi:10.1002/grl.50488.
- Zavala, C., and Arcuri, M., 2016, Intra-basinal and extrabasinal turbidites: Origin and distinctive characteristics: *Sedimentary Geology*, v. 337, p. 36–54, doi:10.1016/j.sedgeo.2016.03.008.
- Zavala, C., Arcuri, M., Di Meglio, M., Diaz, H.G., and Contreras, C., 2011, A genetic facies tract for the analysis of sustained hyperpycnal flow deposits, in Slatt, R.M., and Zavala, C., eds., *Sediment transfer from shelf to deep water—Revisiting the delivery system*: American Association of Petroleum Geologists Studies in Geology 61, p. 31–51, doi:10.1306/13271349St613438.

Manuscript received 4 August 2016

Revised manuscript received 19 September 2016

Manuscript accepted 17 October 2016

Printed in USA